Journal of Non-Crystalline Solids 363 (2013) 39–45

Contents lists available at SciVerse ScienceDirect

Journal of Non-Crystalline Solids

journal homepage: www.elsevier.com/ locate/ jnoncrysol

Liquidus surface of $MgO–CaO–Al_2O_3–SiO_2$ glass-forming systems

Brett M. Abel, John C. Mauro *, Morten M. Smedskjaer [1], James M. Morgan, Christopher L. LaPierre, Gary R. Swan, Mark E. Mack, Adam J. Ellison

Science and Technology Division, Corning Incorporated, Corning, NY 14831, USA

ARTICLE INFO

Article history:
Received 2 November 2012
Received in revised form 12 December 2012
Available online 9 January 2013

Keywords:
Silicates;
Magnesium oxide;
Calcium oxide;
Liquidus temperature

ABSTRACT

Alkaline earth aluminosilicate systems are of widespread technological importance, and it is therefore essential to have accurate phase equilibrium diagrams available. While the phase equilibria for the single alkaline earth $CaO–Al_2O_3–SiO_2$ and $MgO–Al_2O_3–SiO_2$ systems are fairly well established, the mixed $MgO–CaO–Al_2O_3–SiO_2$ systems have received little attention despite their important role in the high-tech glass industry. Here, the liquidus surface (liquidus temperature T_{liq} and primary devitrification phase) is determined by x-ray diffraction phase analyses of isothermally reacted samples from powder mixtures. The phase equilibrium diagrams are presented based on measurements on a total of 120 compositions. In the composition range of interest for industrial glasses, T_{liq} tends to increase with increasing silica content and decreasing alkaline earth-to-alumina ratio. Cristobalite, mullite, anorthite, and cordierite are found to be the dominant devitrification phases for the compositions with high SiO_2, Al_2O_3, CaO, and MgO contents, respectively. Anorthite extends further into the cristobalite and mullite fields for the [CaO]/[MgO] = 3 system compared to the cordierite behavior in systems with [MgO]/[CaO] = 3. For systems with [MgO] = [CaO], the liquidus temperatures are shifted to lower values since the formation of anorthite and cordierite requires some critical concentration of CaO and MgO, respectively.

1. Introduction

Fundamental questions in relation to understanding the structure, dynamics, and properties of oxide glasses have been studied for nearly 100 years [1]. Indeed, oxide glasses continue to play an important role in current and emerging technologies. For example, they are applied as liquid crystal display substrates [2], radioactive waste glasses [3], bioactive glasses for regeneration of bone and tissues in the human body [4], and chemically strengthened glass covers for personal electronic devices [5]. While some chemical compositions may result in the optimum thermal, mechanical, optical, and/or chemical properties for a given application, the glass forming ability (GFA) of such compositions may not be sufficiently high to allow for continuous industrial glass production. Industrial oxide glasses are typically prepared by the melt quenching method, where the mixed raw materials are first melted at a temperature above their liquidus temperature and then cooled sufficiently quickly to avoid crystallization. The glass forming ability (GFA), i.e., the minimum critical cooling rate to obtain a glass with a crystalline fraction below a certain limit, depends on the melt composition [6]. Hence, it is important to understand the connection between chemical composition and GFA [7].

Fortunately, the GFA is strongly correlated with the liquidus viscosity (η_{liq}) of the system, which is the equilibrium viscosity of the liquid at its liquidus temperature (T_{liq}) [8]. T_{liq} is the highest temperature of thermodynamic equilibrium between the solid and liquid phases, above which crystals of any kind are thermodynamically unstable. A low value of T_{liq} generally results in a high value of η_{liq}, and hence a large kinetic barrier to the atomic rearrangements necessary for crystallization. This explains the direct connection between GFA and η_{liq}, and the best glass-formers are thus typically found around eutectic compositions. It is therefore important to have accurate knowledge of phase equilibrium diagrams for the glass-forming systems of commercial interest. Both thermodynamic [9–14] and empirical [15,16] methods exist for predicting T_{liq} based on chemical composition. However, thermodynamic data are often unavailable, and it is difficult to extrapolate empirical models out of the range of the previous experiments. Furthermore, while some thermodynamic models can accurately reproduce binary phase diagrams [17], their ability to predict multicomponent properties based on information from the binary systems is much more limited [17,18]. Therefore, for most systems of industrial interest, T_{liq} as a function of composition is traditionally determined experimentally, despite the fact that it is difficult and time-consuming, particularly for good glass-forming systems [19]. However, it should be noted that Ferreira et al. have recently developed a fast differential scanning calorimetry (DSC) method to estimate T_{liq} [20].

Alkaline earth aluminosilicate glasses constitute a particularly important class of compositions due to their use as active matrix liquid crystal display (AMLCD) substrates [2]. This is because these glasses possess the suitable combination of thermal and mechanical stability required for AMLCD substrates. Moreover, the glasses used as substrate

* Corresponding author. Tel.: +1 607 974 2185.
E-mail address: mauroj@corning.com (J.C. Mauro).
[1] Present address: Section of Chemistry, Aalborg University, Denmark.

0022-3093/$ – see front matter © 2012 Elsevier B.V. All rights reserved.
http://dx.doi.org/10.1016/j.jnoncrysol.2012.12.020

materials must have no inclusions large enough to interfere with pixels in the final display, and they must be essentially free of alkali oxides to ensure that they do not interact with the thin-film transistors [2,21]. The phase equilibrium diagrams for the single alkaline earth CaO–Al_2O_3–SiO_2 [13,22–24] and MgO–Al_2O_3–SiO_2 [25–27] systems have been widely studied in literature. However, the parts of these phase diagrams of highest industrial interest need to be explored in greater detail. For example, our experiments indicate some doubt about the existence of tridymite (a high-temperature polymorph of quartz) in the high-SiO_2 compositions. Furthermore, the mixed MgO–CaO–Al_2O_3–SiO_2 quaternary systems have received little attention despite their great technological importance.

In this paper, the phase equilibria (liquidus temperature and primary devitrification phase) are therefore determined for a total of 120 compositions within the MgO–CaO–Al_2O_3–SiO_2 system. Focus is on the compositional regions of commercial interest for industrial glass production, i.e., compositions with SiO_2 content around 60–75 mol% and Al_2O_3 content around 10–15 mol%. The compositions were designed in order to center them around the known cristobalite phase boundary. Finally, the phase equilibrium diagrams are summarized and discussed.

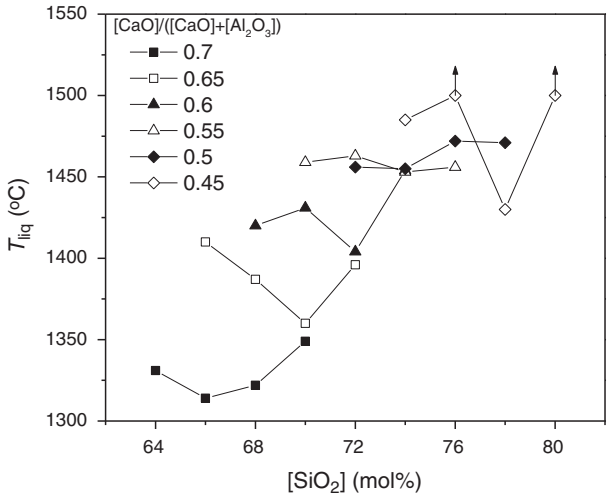

Fig. 1. Liquidus temperature (T_{liq}) as a function of the SiO_2 concentration in the CaO–Al_2O_3–SiO_2 system for different [CaO]/[Al_2O_3] ratios. The arrows indicate that the data points represent lower limits of T_{liq}. The error range of T_{liq} is around ±10–15 K.

2. Experimental procedure

Powders of MgO (Penoles Metals and Chemicals, 0.993 purity), CaO (Avantor, 0.9995 purity), Al_2O_3 (ALFA Aesar, 0.9999 purity), and SiO_2 (Index Minerals Processor, 0.99966 purity) were prepared in 200 g batches for 120 different compositions. The materials were weighed into a ½ gallon (2.2 liter) Nalgene container, after which 6.5 inch (12.7 mm) diameter high purity alumina balls were added to the container and then placed into a Turbula-type mixer. After 30 minutes of mixing the alumina balls were removed from the Nalgene container. The compositions stated in the tables below are all nominal (as-batched). The potential errors due to weighing uncertainty are less than 0.1 mol%.

Table 1
Liquidus temperature (T_{liq}) and devitrification phase(s) at T_{liq} for the CaO–Al_2O_3–SiO_2 system. The error range of T_{liq} is around ±10–15 K.

Composition (mol%)			[CaO]/([CaO]+[Al_2O_3])	T_{liq} (°C)	Devitrification phase[a]
SiO_2	Al_2O_3	CaO			
64	10.8	25.2	0.7	1331	Crist
66	10.2	23.8	0.7	1314	Crist + An
68	9.6	22.4	0.7	1322	Crist
70	9	21	0.7	1349	Crist
66	11.9	22.1	0.65	1410	An
68	11.2	20.8	0.65	1387	An
70	10.5	19.5	0.65	1360	Crist
72	9.8	18.2	0.65	1396	Crist
68	12.8	19.2	0.6	1420	An
70	12	18	0.6	1431	An
72	11.2	16.8	0.6	1404	Crist
74	10.4	15.6	0.6	1454	Crist
70	13.5	16.5	0.55	1459	An
72	12.6	15.4	0.55	1463	An + Crist
74	11.7	14.3	0.55	1453	Crist
76	10.8	13.2	0.55	1456	Crist
72	14	14	0.5	1456	An + Cor
74	13	13	0.5	1455	Crist
76	12	12	0.5	1472	Crist
78	11	11	0.5	1471	Crist
74	14.3	11.7	0.45	1485	Mu
76	13.2	10.8	0.45	>1500	Mu
78	12.1	9.9	0.45	1430	Crist + Qu
80	11	9	0.45	>1500	Crist

[a] An: anorthite ($CaAl_2Si_2O_8$); Cor: corundum (Al_2O_3); Crist: cristobalite (SiO_2); Mu: mullite ($Al_6Si_2O_{13}$); Qu: quartz (SiO_2).

Small (~5 g) samples of the mixed powders were heated isothermally at different temperatures for 72 h. The temperatures were varied between 1250 and 1500 °C in 25 °C steps. The heat-treatments were performed in a furnace heated using molydisilicide heating elements. The temperature was controlled within ±5–7 °C using the B-type thermocouple, which was placed right next to the samples. After the samples had been heat-treated for 72 h, they were quickly quenched by removing them from the furnace.

The samples were then analyzed using x-ray diffraction (XRD) to determine the crystallinity of the samples and identify any crystalline phases present. The samples were prepared for XRD analysis by grinding to a fine powder using a Rocklabs ring mill. The powder was then pressed into a standard top loaded sample holder. Using a Bruker D4 Endeavor equipped with a LynxEye™ silicon strip detector, scan data was collected from 5° to 80° (2θ). Analyses of the resulting scans were completed with the use of the PDF-4 database and Jade. The database is a product of the International Centre for Diffraction Data (ICDD®). Jade

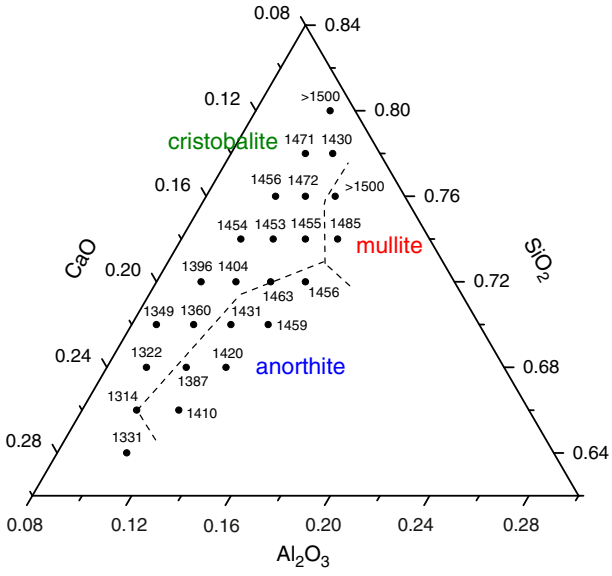

Fig. 2. Phase diagram for the CaO–Al_2O_3–SiO_2 system based on the experimental data in Table 1. The numbers indicate the liquidus temperatures (in °C) and dashed lines the estimated phase boundaries. The oxide concentrations are expressed in mole fraction units.

is a search match program produced by Materials Data Incorporated (MDI). Crystalline phases were identified based on peak locations, peak intensities, and the chemical information provided.

3. Results and discussion

The liquidus temperature of each composition is determined as the temperature at which the final crystals melt upon heating. Isothermal holds are performed at 25 °C intervals and then obtained the XRD pattern. T_{liq} is thus often somewhere in between two temperatures (e.g., 1325 and 1350 °C), when the low temperature XRD pattern exhibits crystalline peaks and the high temperature XRD pattern exhibits only amorphous features. In order to estimate T_{liq}, the crystalline peak intensities are extrapolated from lower to higher temperatures. T_{liq} corresponds to the temperature at which the intensity of the crystalline peaks is found to be zero. The primary devitrification phase(s) is/are the crystalline phase(s) identified in the XRD pattern for the highest temperature sample still containing crystals. With the obtained information about T_{liq} and primary devitrification phase(s), the phase equilibrium diagrams can be drawn. The phase boundary lines are drawn through the experimental data points when two or more devitrification phases co-exist.

In the following sections, the experimental results for the three investigated systems ($CaO–Al_2O_3–SiO_2$, $MgO–Al_2O_3–SiO_2$, and mixed $MgO–CaO–Al_2O_3–SiO_2$) are presented and discussed.

3.1. $CaO–Al_2O_3–SiO_2$ system

The investigated compositions and determined liquidus temperatures and devitrification phases for the $CaO–Al_2O_3–SiO_2$ system are given in Table 1. The compositions are designed with six different $[CaO]/[Al_2O_3]$ ratios for four different SiO_2 concentrations at each $[CaO]/[Al_2O_3]$ ratio. Fig. 1 shows that T_{liq} generally decreases with increasing $[CaO]/[Al_2O_3]$ ratio. Moreover, for each $[CaO]/[Al_2O_3]$ ratio, there appears to be a local minimum of T_{liq} for an intermediate SiO_2 content.

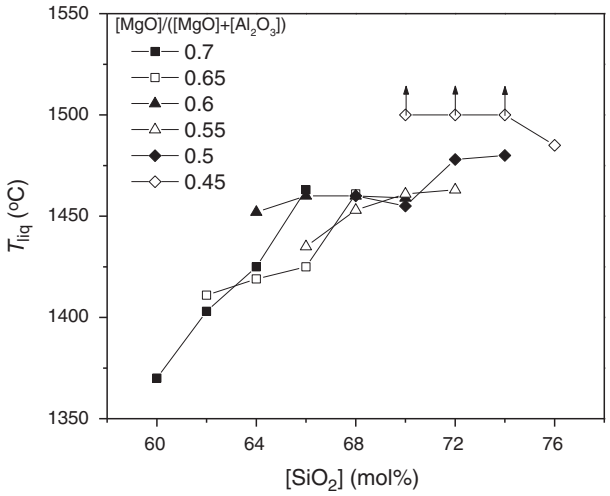

Fig. 3. Liquidus temperature (T_{liq}) as a function of the SiO_2 concentration in the $MgO–Al_2O_3–SiO_2$ system for different $[MgO]/[Al_2O_3]$ ratios. The arrows indicate that the data points represent lower limits of T_{liq}. The error range of T_{liq} is around ±10–15 K.

Based on the data in Table 1, the phase equilibrium diagram for the $CaO–Al_2O_3–SiO_2$ system is drawn for $[SiO_2]$ between 64 and 80 mol%, $[Al_2O_3]$ between 9 and 14.3 mol%, and [CaO] between 9 and 25.2 mol%. The diagram is shown in Fig. 2. Anorthite ($CaAl_2Si_2O_8$), cristobalite (SiO_2), and mullite ($Al_6Si_2O_{13}$) are the dominant crystalline phases in this composition range.

3.2. $MgO–Al_2O_3–SiO_2$ system

The experimental results for the $MgO–Al_2O_3–SiO_2$ system are given in Table 2. The compositions within this system are designed in a similar manner as those in the $CaO–Al_2O_3–SiO_2$ system with six different $[MgO]/[Al_2O_3]$ ratios. However, the silica content is systematically lowered by 4 mol%. T_{liq} increases with increasing $[SiO_2]$ and decreasing $[MgO]/[Al_2O_3]$ ratio (Fig. 3). The ternary phase equilibrium

Table 2
Liquidus temperature (T_{liq}) and devitrifaction phase(s) at T_{liq} for the $MgO–Al_2O_3–SiO_2$ system. The error range of T_{liq} is around ±10–15 K.

Composition (mol%)			[MgO]/([MgO]+[Al2O3])	Tliq (°C)	Devitrification phase[a]
SiO2	Al2O3	MgO			
60	12	28	0.7	1370	Cord + Crist + Qu
62	11.4	26.6	0.7	1403	Tr
64	10.8	25.2	0.7	1425	Tr
66	10.2	23.8	0.7	1463	Crist
62	13.3	24.7	0.65	1411	Cord
64	12.6	23.4	0.65	1419	Cord + Tr
66	11.9	22.1	0.65	1425	Cord + Crist + Tr
68	11.2	20.8	0.65	1461	Crist
64	14.4	21.6	0.6	1452	Crist
66	13.6	20.4	0.6	1460	Crist
68	12.8	19.2	0.6	1460	Crist
70	12	18	0.6	1459	Crist
66	15.3	18.7	0.55	1435	Cord + Crist
68	14.4	17.6	0.55	1453	Crist
70	13.5	16.5	0.55	1461	Crist
72	12.6	15.4	0.55	1463	Crist
68	16	16	0.5	1460	Mu
70	15	15	0.5	1455	Crist + Mu
72	14	14	0.5	1478	Crist
74	13	13	0.5	1480	Crist
70	16.5	13.5	0.45	>1500	Mu
72	15.4	12.6	0.45	>1500	Mu
74	14.3	11.7	0.45	>1500	Mu
76	13.2	10.8	0.45	1485	Mu

[a] Cord: cordierite ($Mg_2Al_4Si_5O_{18}$); Crist: cristobalite (SiO_2); Mu: mullite ($Al_6Si_2O_{13}$); Qu: quartz (SiO_2); Tr: tridymite (SiO_2).

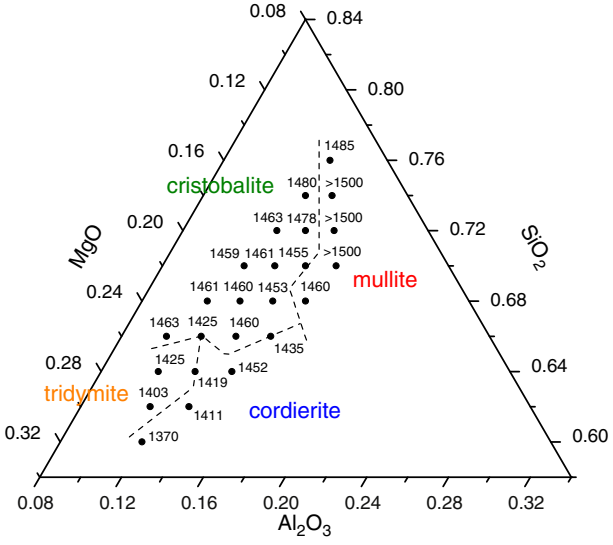

Fig. 4. Phase diagram for the $MgO–Al_2O_3–SiO_2$ system based on the experimental data in Table 2. The numbers indicate the liquidus temperatures (in °C) and dashed lines the estimated phase boundaries. The oxide concentrations are expressed in mole fraction units.

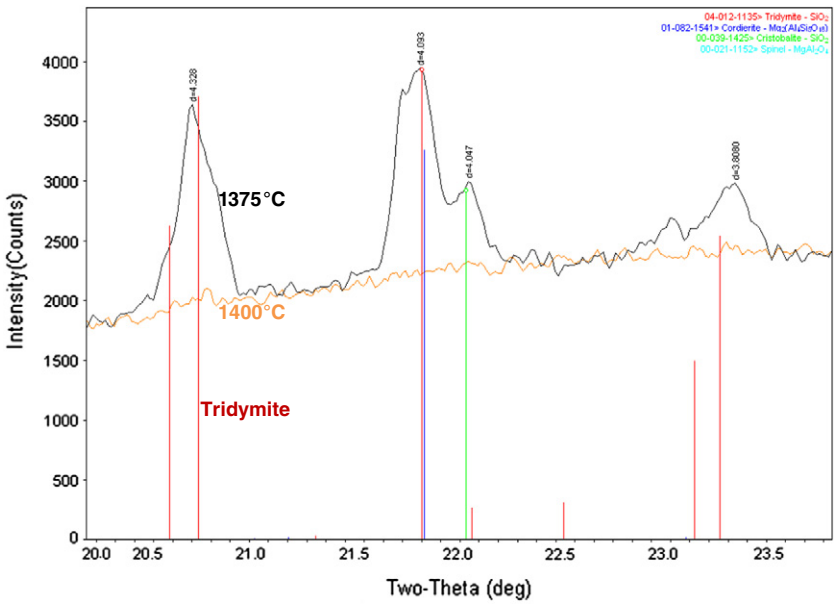

Fig. 5. XRD spectra for 26.6MgO–11.4Al_2O_3–62SiO_2 (mol%) after 72-h isothermal treatments at 1375 and 1400 °C. The MgO–Al_2O_3–SiO_2 system showing clear evidence of tridymite as a primary devitrification phase.

diagram for this system is shown in Fig. 4. In addition to cristobalite and mullite, this system also has tridymite (SiO_2) and cordierite ($Mg_2Al_4Si_5O_{18}$) as the equilibrium crystalline phases. It is interesting to note that tridymite appears as a primary devitrification phase of SiO_2 in the MgO–Al_2O_3–SiO_2 system (Fig. 5), whereas the CaO–Al_2O_3–SiO_2 system displays cristobalite as the only SiO_2 phase (Fig. 6). In comparison with the CaO-based system, the MgO-based system also has higher liquidus temperatures, especially for the regime of low Al_2O_3 contents.

3.3. *CaO–MgO–Al_2O_3–SiO_2 system*

The mixed CaO–MgO–Al_2O_3–SiO_2 system has been prepared with three different [MgO]/[CaO] ratios equal to 3, 1, and 1/3. Figs. 7 and 8 show the composition dependence of T_{liq} and the phase equilibrium diagram, respectively, for [MgO]/[CaO] = 3 system. The data are also presented in Table 3. T_{liq} increases with increasing [SiO_2], in accordance with the results for the single alkaline earth systems. However, unlike these systems, T_{liq} does not increase systematically with decreasing [RO]/[Al_2O_3] ratio, where [RO] = [MgO] + [CaO] (Fig. 7). The major crystalline phases present in this system are cristobalite, mullite, and cordierite. Hence, when [MgO]/[CaO] = 3, cordierite suppresses the formation of anorthite.

When the concentration of CaO is three times higher than that of MgO (Table 4), the liquidus temperature does not monotonically increase with [SiO_2]. As shown in Fig. 9, a local minimum in T_{liq} is instead observed for some [RO]/[Al_2O_3] ratios. Moreover, T_{liq} generally increases with increasing [RO]/[Al_2O_3] ratio (Fig. 9). It should also be

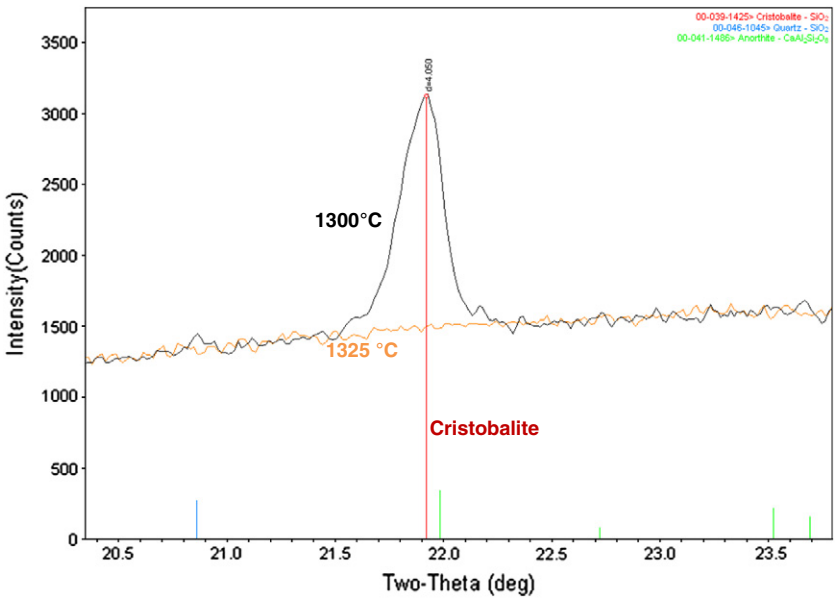

Fig. 6. XRD spectra for 22.4CaO–9.6Al_2O_3–68SiO_2 (mol%) after 72-h isothermal treatments at 1325 and 1300 °C. In contrast to the MgO–Al_2O_3–SiO_2 system, here there is no evidence for formation of tridymite. Rather, the primary silica devitrification phase is cristobalite.

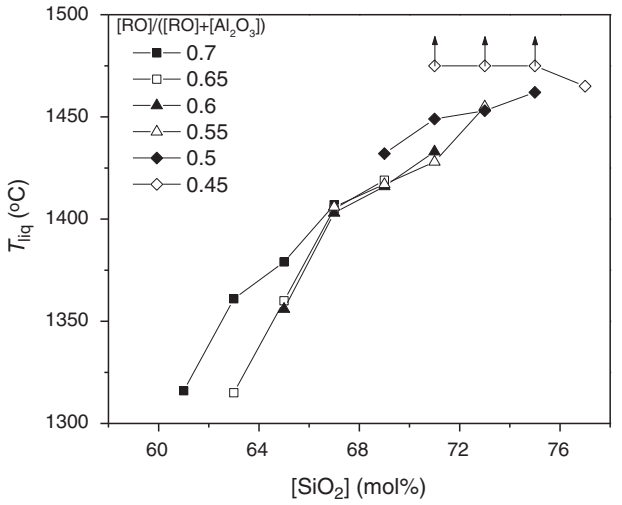

Fig. 7. Liquidus temperature (T_{liq}) as a function of the SiO_2 concentration in the MgO–CaO–Al_2O_3–SiO_2 system with [MgO]/[CaO] = 3 for different [RO]/[Al_2O_3] ratios, where [RO] = [MgO] + [CaO]. The arrows indicate that the data points represent lower limits of T_{liq}. The error range of T_{liq} is around ±10–15 K.

noted that anorthite field extends further into the cristobalite and mullite fields than cordierite does for the system with [MgO]/[CaO] = 3 (Fig. 10).

For [MgO] = [CaO] system, the liquidus temperature is generally shifted to lower values compared to the system with [MgO]/[CaO] = 3 (Table 5). For low silica contents (~62–70 mol%), T_{liq} increases with increasing [RO]/[Al_2O_3] ratio (Fig. 11). This system is dominated by cristobalite as the equilibrium phase for most of the studied compositions (Fig. 12). Cristobalite extends into the composition range that was dominated by anorthite or cordierite in the systems mentioned in the above. Hence, the formation of anorthite and cordierite requires some critical concentration of CaO and MgO, respectively. This shifts the liquidus temperature to lower values for the mixed MgO–CaO system compared with the single alkaline earth systems. As mentioned in the introduction section, this is important when designing melt compositions with high GFA.

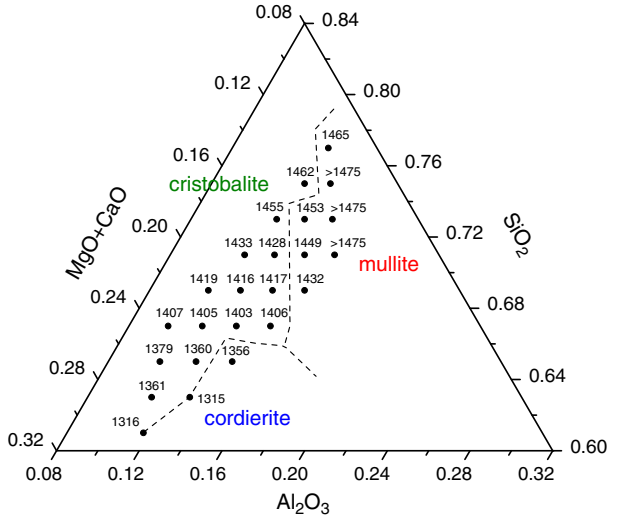

Fig. 8. Phase diagram for the MgO–CaO–Al_2O_3–SiO_2 system with [MgO]/[CaO] = 3 based on the experimental data in Table 3. The numbers indicate the liquidus temperatures (in °C) and dashed lines the estimated phase boundaries. The oxide concentrations are expressed in mole fraction units.

Table 3
Liquidus temperature (T_{liq}) and devitrification phase(s) at T_{liq} for the MgO–CaO–Al_2O_3–SiO_2 system with [MgO]/[CaO] = 3. The error range of T_{liq} is around ±10–15 K.

Composition (mol%)				[RO]/([RO] + [Al_2O_3])	T_{liq} (°C)	Devitrification phase[a]
SiO_2	Al_2O_3	CaO	MgO			
61	11.7	6.83	20.48	0.7	1316	Crist + Cord
63	11.1	6.48	19.43	0.7	1361	Crist
65	10.5	6.13	18.38	0.7	1379	Crist
67	9.9	5.78	17.33	0.7	1407	Crist
63	12.95	6.01	18.04	0.65	1315	Crist + Cord
65	12.25	5.69	17.06	0.65	1360	Crist
67	11.55	5.36	16.09	0.65	1405	Crist
69	10.85	5.04	15.11	0.65	1419	Crist
65	14	5.25	15.75	0.6	1356	Cord
67	13.2	4.95	14.85	0.6	1403	Crist
69	12.4	4.65	13.95	0.6	1416	Crist
71	11.6	4.35	13.05	0.6	1433	Crist
67	14.85	4.54	13.61	0.55	1406	Crist
69	13.95	4.26	12.79	0.55	1417	Crist
71	13.05	3.99	11.96	0.55	1428	Crist
73	12.15	3.71	11.14	0.55	1455	Crist
69	15.5	3.88	11.63	0.5	1432	Mu
71	14.5	3.63	10.88	0.5	1449	Mu
73	13.5	3.38	10.13	0.5	1453	Mu
75	12.5	3.13	9.38	0.5	1462	Crist
71	15.95	3.26	9.79	0.45	>1475	Mu
73	14.85	3.04	9.11	0.45	>1475	Mu
75	13.75	2.81	8.44	0.45	>1475	Mu
77	12.65	2.59	7.76	0.45	1465	Mu

[a] Cord: cordierite ($Mg_2Al_4Si_5O_{18}$); Crist: cristobalite (SiO_2); Mu: mullite ($Al_6Si_2O_{13}$).

4. Conclusions

The phase relationships in the single alkaline earth and mixed CaO/MgO–Al_2O_3–SiO_2 systems have been investigated, emphasizing the regions of greatest commercial interest for AMLCD glass substrate compositions. The compositions with high silica and low alumina content are found to be dominated by cristobalite, whereas tridymite

Table 4
Liquidus temperature (T_{liq}) and devitrification phase(s) at T_{liq} for the MgO–CaO–Al_2O_3–SiO_2 system with [CaO]/[MgO] = 3. The error range of T_{liq} is around ±10–15 K.

Composition (mol%)				[RO]/([RO] + [Al_2O_3])	T_{liq} (°C)	Devitrification phase[a]
SiO_2	Al_2O_3	CaO	MgO			
63	11.1	19.43	6.48	0.7	1309	Crist + An
65	10.5	18.38	6.13	0.7	1305	Crist + An
67	9.9	17.33	5.78	0.7	1354	Crist
69	9.3	16.28	5.43	0.7	1407	Crist + Qu
65	12.25	17.06	5.69	0.65	1327	An
67	11.55	16.09	5.36	0.65	1334	An
69	10.85	15.11	5.04	0.65	1366	Crist
71	10.15	14.14	4.71	0.65	1402	Crist
67	13.2	14.85	4.95	0.6	1353	An
69	12.4	13.95	4.65	0.6	1321	Crist + Qu + An
71	11.6	13.05	4.35	0.6	1365	Crist + Qu
73	10.8	12.15	4.05	0.6	1413	Crist
69	13.95	12.79	4.26	0.55	1331	Crist + An
71	13.05	11.96	3.99	0.55	1359	Crist + Qu
73	12.15	11.14	3.71	0.55	1388	Crist + Qu
75	11.25	10.31	3.44	0.55	1419	Crist + Qu
71	14.5	10.88	3.63	0.5	1369	Crist + An + Qu
73	13.5	10.13	3.38	0.5	1380	Crist + Qu + An
75	12.5	9.38	3.13	0.5	1416	Crist + Qu
77	11.5	8.63	2.88	0.5	1435	Crist + Qu
73	14.85	9.11	3.04	0.45	>1450	Mu
75	13.75	8.44	2.81	0.45	1414	Crist + Mu + Qu
77	12.65	7.76	2.59	0.45	1429	Crist + Qu + Mu
79	11.55	7.09	2.36	0.45	1453	Crist

[a] An: anorthite ($CaAl_2Si_2O_8$); Crist: cristobalite (SiO_2); Mu: mullite ($Al_6Si_2O_{13}$); Qu: quartz (SiO_2).

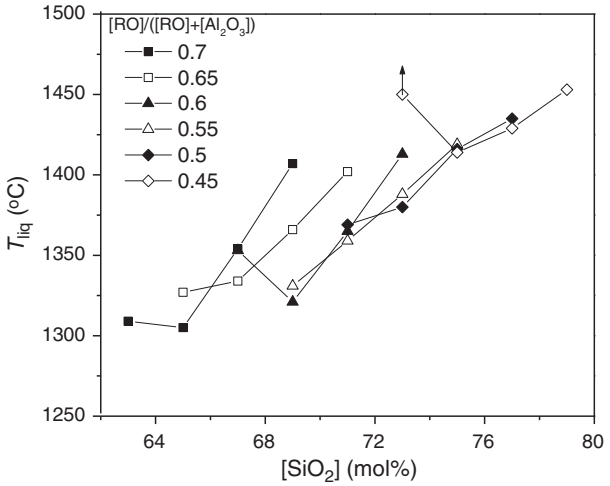

Fig. 9. Liquidus temperature (T_{liq}) as a function of the SiO_2 concentration in the MgO–CaO–Al_2O_3–SiO_2 system with [CaO]/[MgO] = 3 for different [RO]/[Al_2O_3] ratios, where [RO] = [MgO] + [CaO]. The arrow indicates that the data point represents the lower limit of T_{liq}. The error range of T_{liq} is around ±10–15 K.

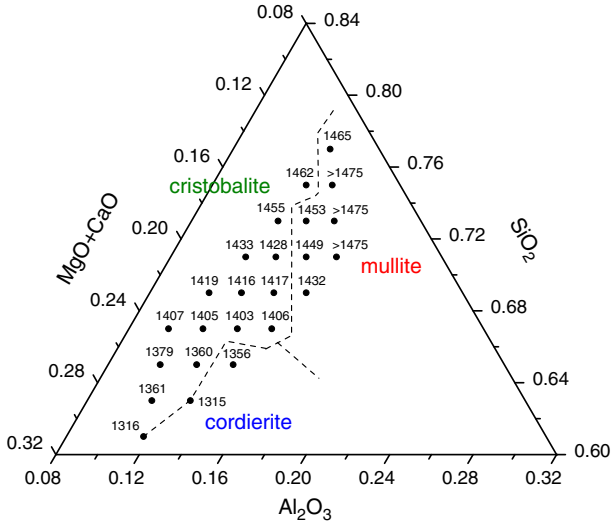

Fig. 10. Phase diagram for the MgO–CaO–Al_2O_3–SiO_2 system with [CaO]/[MgO] = 3 based on the experimental data in Table 4. The numbers indicate the liquidus temperatures (in °C) and dashed lines the estimated phase boundaries. The oxide concentrations are expressed in mole fraction units.

is only found in the MgO–Al_2O_3–SiO_2 system. The mixing of MgO and CaO is found to shift the liquidus temperature to lower values by suppressing the formation of anorthite and cordierite. Based on the new findings presented here, the composition and production of glass substrates for AMLCD belonging to the CaO–MgO–Al_2O_3–SiO_2 family may be designed with a more exact control of the glass forming ability by avoiding the regions of high liquidus temperature.

Acknowledgments

The authors appreciate valuable support from Gregory W. Ermold of Corning Incorporated.

References

[1] M.D. Ediger, P. Harrowell, J. Chem. Phys. 137 (2012) 080901.

Table 5
Liquidus temperature (T_{liq}) and equilibrium phase(s) at T_{liq} for the MgO–CaO–Al_2O_3–SiO_2 system with [MgO] = [CaO]. The error range of T_{liq} is around ±10–15 K.

Composition (mol%)				[RO]/([RO] + [Al_2O_3])	T_{liq} (°C)	Devitrification phase[a]
SiO_2	Al_2O_3	CaO	MgO			
62	11.4	13.3	13.3	0.7	1280	Crist + Qu
64	10.8	12.6	12.6	0.7	1304	Crist + Qu
66	10.2	11.9	11.9	0.7	1361	Crist
68	9.6	11.2	11.2	0.7	1374	Crist
64	12.6	11.7	11.7	0.65	1308	Crist + An
66	11.9	11.05	11.05	0.65	1337	Crist
68	11.2	10.4	10.4	0.65	1363	Crist
70	10.5	9.75	9.75	0.65	1405	Crist
66	13.6	10.2	10.2	0.6	1325	Crist
68	12.8	9.6	9.6	0.6	1354	Crist
70	12	9	9	0.6	1401	Crist
72	11.2	8.4	8.4	0.6	1427	Crist
68	14.4	8.8	8.8	0.55	1356	Crist + Qu
70	13.5	8.25	8.25	0.55	1365	Crist
72	12.6	7.7	7.7	0.55	1412	Crist
74	11.7	7.15	7.15	0.55	1428	Crist
70	15	7.5	7.5	0.5	1426	Mu
72	14	7	7	0.5	1420	Crist + Mu
74	13	6.5	6.5	0.5	1427	Crist + Mu
76	12	6	6	0.5	1438	Crist
72	15.4	6.3	6.3	0.45	>1475	Mu
74	14.3	5.85	5.85	0.45	>1450	Mu
76	13.2	5.4	5.4	0.45	>1450	Mu
78	12.1	4.95	4.95	0.45	>1450	Crist + Qu

[a] An: anorthite ($CaAl_2Si_2O_8$); Crist: cristobalite (SiO_2); Mu: mullite ($Al_6Si_2O_{13}$); Qu: quartz (SiO_2).

[2] A. Ellison, I.A. Cornejo, Int. J. Appl. Glass Sci. 1 (2010) 87.
[3] C.M. Jantzen, K.G. Brown, J.B. Pickett, Int. J. Appl. Glass Sci. 1 (2010) 38.
[4] L.L. Hench, J. Mater. Sci.: Mater. Med. 17 (2006) 967.
[5] A.K. Varshneya, Int. J. Appl. Glass Sci. 1 (2010) 131.
[6] D.R. Uhlmann, J. Non-Cryst. Solids 7 (1972) 337.
[7] Q.J. Zheng, M.M. Smedskjaer, R.E. Youngman, M. Potuzak, J.C. Mauro, Y.Z. Yue, Appl. Phys. Lett. 101 (2012) 041906.
[8] W. Kauzmann, Chem. Rev. 43 (1948) 219.
[9] Q. Rao, G.F. Piepel, P. Hrma, J.V. Crum, J. Non-Cryst. Solids 220 (1997) 17.
[10] C. Dreyfus, G. Dreyfus, J. Non-Cryst. Solids 318 (2003) 63.
[11] V.N. Makanov, I.V. Makarova, O.V. Suvorova, A.N. Sakharchenko, Glass Ceram. 59 (2002) 80.
[12] I.-H. Jung, S.A. Decterov, A.D. Pelton, J. Phase Equilib. Diffus. 25 (2004) 329.
[13] H. Mao, M. Hillert, M. Selleby, B. Sundman, J. Am. Ceram. Soc. 89 (2006) 298.
[14] H. Mao, M. Selleby, B. Sundman, J. Am. Ceram. Soc. 88 (2005) 2544.
[15] R.G.C. Beerkens, R. Conradt, Glass Technol. Eur. J. Glass Sci. Technol. A 49 (2008) 205.

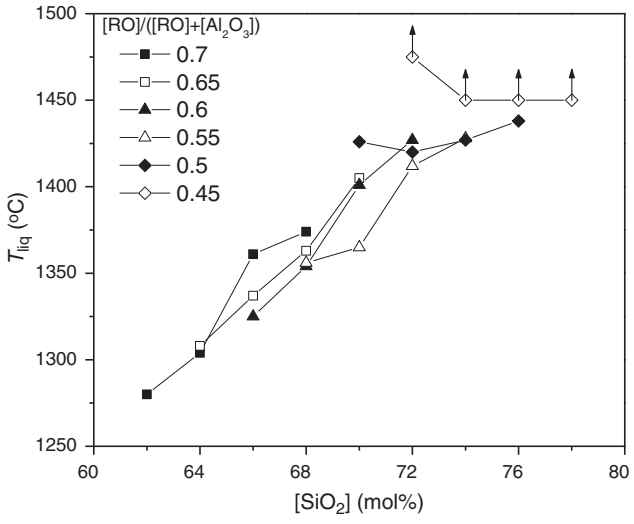

Fig. 11. Liquidus temperature (T_{liq}) as a function of the SiO_2 concentration in the MgO–CaO–Al_2O_3–SiO_2 system with [MgO] = [CaO] for different [RO]/[Al_2O_3] ratios, where [RO] = [MgO] + [CaO]. The arrows indicate that the data points represent lower limits of T_{liq}. The error range of T_{liq} is around ±10–15 K.

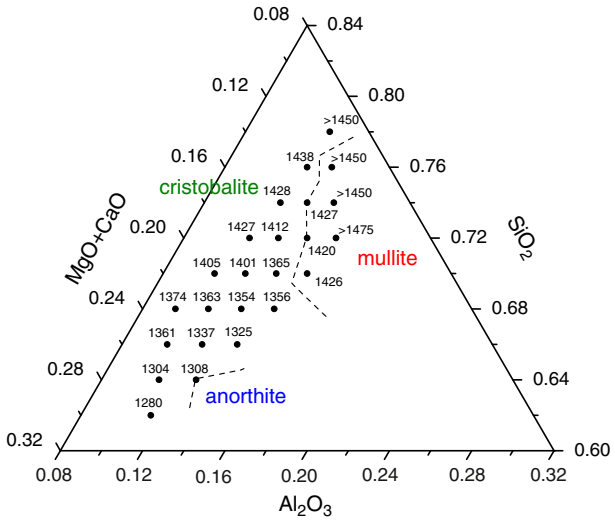

Fig. 12. Phase diagram for the MgO–CaO–Al_2O_3–SiO_2 system with [MgO] = [CaO] based on the experimental data in Table 5. The numbers indicate the liquidus temperatures (in °C) and dashed lines the estimated phase boundaries. The oxide concentrations are expressed in mole fraction units.

[16] A. Fluegel, Glass Liquidus Temperature Calculation. Available at http://glassproperties.com/liquidus/, (accessed July 6, 2012).
[17] I.-H. Jung, Calphad 34 (2010) 332.
[18] D.-P. Tao, Metall. Mater. Trans. B 43 (2012) 1247.
[19] F.T. Wallenberger, A. Smrcek, Int. J. Appl. Glass Sci. 1 (2010) 151.
[20] E.B. Ferreira, M.L. Lima, E.D. Zanotto, J. Am. Ceram. Soc. 93 (2010) 3757.
[21] A.J. Ellison, T.J. Kiczenski, U.S. Patent Application No. 2012/0088648 A1, 2012.
[22] E.F. Osborn, A. Muan, Phase Equilibrium Diagrams of Oxide Systems, Plate 1, The System CaO–Al_2O_3–SiO_2, American Ceramic Society and Edward Orton, Ir., Ceramic Foundation, Columbus, OH, 1960.
[23] G.A. Rankin, F.E. Wright, Am. J. Sci. 39 (1915) 1.
[24] J.R. Goldsmith, J. Geol. 15 (1947) 383.
[25] E.M. Levin, C.R. Robbins, H.F. McMurdie, Phase Diagrams for Ceramists, American Ceramic Society, Columbus, OH, 1964.
[26] W. Schreyer, J.F. Schairer, Am. Mineral. 47 (1962) 90.
[27] C.M. Schlaudt, D.M. Roy, J. Am. Ceram. Soc. 48 (1965) 248.